C. R. Physique 20 (2019) 176–182

Contents lists available at ScienceDirect

Comptes Rendus Physique

www.sciencedirect.com

URSI-France 2018 Workshop: Geolocation and navigation / *Journées URSI-France 2018 : géolocalisation et navigation*

A new test of gravitational redshift using Galileo satellites: The GREAT experiment

Un nouveau test de décalage gravitationnel vers le rouge à l'aide des satellites Galileo : l'expérience GREAT

Pacôme Delva [a,*], Neus Puchades [a,b], Erik Schönemann [c], Florian Dilssner [c], Clément Courde [d], Stefano Bertone [e], Francisco Gonzalez [f], Aurélien Hees [a], Christophe Le Poncin-Lafitte [a], Frédéric Meynadier [a], Roberto Prieto-Cerdeira [f], Benoît Sohet [a], Javier Ventura-Traveset [g], Peter Wolf [a]

[a] *SYRTE, Observatoire de Paris, Université PSL, CNRS, Sorbonne Université, LNE, 61, avenue de l'Observatoire, 75014 Paris, France*
[b] *Departamento de Astronomía y Astrofísica, Edificio de Investigación Jerónimo Muñoz, C/Dr. Moliner, 50, 46100 Burjassot (Valencia), Spain*
[c] *European Space Operations Center, ESA/ESOC, Darmstadt, Germany*
[d] *UMR Geoazur, Université de Nice, Observatoire de la Côte d'Azur, 250, rue Albert-Einstein, 06560 Valbonne, France*
[e] *Astronomical Institute, University of Bern, Sidlerstrasse 5, CH-3012 Bern, Switzerland*
[f] *European Space and Technology Centre, ESA/ESTEC, Noordwijk, The Netherlands*
[g] *European Space and Astronomy Center, ESA/ESAC, Villanueva de la Cañada, Spain*

ARTICLE INFO

Article history:
Available online 9 May 2019

Keywords:
GNSS
Galileo
General Relativity
Gravitational Redshift
Equivalence Principle

Mots-clés :
GNSS
Galileo
Relativité Générale
Décalage Gravitationnel vers le rouge
Principe d'Équivalence

ABSTRACT

We present the result of the analysis of the GREAT (Galileo gravitational Redshift test with Eccentric sATellites) experiment. An elliptic orbit induces a periodic modulation of the fractional frequency difference between a ground clock and the satellite clock, partly due to the gravitational redshift, while the good stability of Galileo clocks allows one to test this periodic modulation to a high level of accuracy. GSAT0201 and GSAT0202, with their large eccentricity and on-board H-maser clocks, are perfect candidates to perform this test. Satellite laser ranging data allows us to partly decorrelate the orbit perturbations from the clock errors. By analyzing several years of Galileo tracking data, we have been able to improve the Gravity probe A test (1976) of the gravitational redshift by a factor of 5.6, providing, to our knowledge, the first reported improvement since more than 40 years.

RÉSUMÉ

Nous présentons les résultats de l'analyse de l'expérience GREAT (*Galileo gravitational Redshift test with Eccentric sATellites*). Une orbite elliptique induit une modulation périodique de la différence de fréquence relative entre une horloge au sol et l'horloge du satellite, due en partie au décalage gravitationnel vers le rouge, tandis que la bonne stabilité des horloges Galileo permet de tester cette modulation périodique à un niveau élevé de précision. Les satellites GSAT0201 et GSAT0202, avec leur grande excentricité et leurs horloges H-maser

---

[*] Corresponding author.
E-mail address: Pacome.Delva@obspm.fr (P. Delva).

https://doi.org/10.1016/j.crhy.2019.04.002

embarquées, sont des candidats parfaits pour mener à bien ce test. De plus, des données de télémétrie laser sur satellites nous permettent de décorréler partiellement les perturbations de l'orbite et les erreurs d'horloge. En analysant plusieurs années de données de suivi Galileo, nous avons été en mesure d'améliorer le test de Gravity Probe A (1976) du décalage gravitationnel vers le rouge d'un facteur 5.6, fournissant, à notre connaissance, la première amélioration signalée depuis plus de 40 ans.

---

1. Introduction

The classical theory of General Relativity (GR) provides a geometrical description of the gravitational interaction. It is based on two fundamental principles: (i) the Einstein Equivalence Principle (EEP) and (ii) the Einstein field equations that can be derived from the Einstein–Hilbert action. All GR extensions or alternative theories of gravitation will break at least one of these principles. The EEP was first envisioned in 1907 by Albert Einstein in [1], where he says that "we shall therefore assume the complete physical equivalence of a gravitational field and a corresponding acceleration of the reference system". This principle eventually led, after quite some thoughts from renowned physicists and mathematicians, to the development of "metric theories" of gravity, in which (i) spacetime is endowed with a metric; (ii) the worldlines of test bodies are the geodesics of this metric; (iii) EEP is satisfied, with the non-gravitational laws in any freely falling frame reducing to the laws of special relativity (see e.g. [2,3]).

Following Will [4], EEP can be divided into three sub-principles:

- Universality of Free Fall (UFF): if any uncharged test body is placed at an initial event in space-time and given an initial velocity there, then its subsequent trajectory will be independent of its internal structure and composition;
- Local Position Invariance (LPI): The outcome of any local non-gravitational test experiment is independent of where and when in the universe it is performed;
- Local Lorentz Invariance (LLI): The outcome of any local non-gravitational test experiment is independent of the velocity of the (freely falling) apparatus.

These principles can be tested with some apparatus, which can be specially designed for the test or not.

In this article, after a review of the existing and planned tests of LPI, we report on a very recent test of LPI using two eccentric Galileo satellites: GSAT0201 and GSAT0202. While the launch in 2014 of these two satellites was first considered as a failure, we soon realized [5] that they could be used to improve one of the long-standing classical test of GR: the gravitational redshift test of Gravity Probe A rocket, launched in 1976.

2. Local position invariance (LPI)

LPI stipulates that the outcome of any local non-gravitational experiment is independent of the space-time position of the freely falling reference frame in which it is performed (see, e.g., [3]). This principle is mainly tested by two types of experiments: (i) search for variations of the constants of Nature and (ii) redshift tests.

The question of the constancy of the constants of Nature was first addressed by Dirac. This question is driven by the "principle of reason": there should be a reason behind the specific values of the constants of physics (see the discussion in Section 2 of [6]). This argument leads to many developments of extensions of physics where the constants of physics become dynamical entities. In parallel, many observational investigations search for any space/time evolution of the constants of physics (see [7]).

Amongst all the observations performed, atomic clocks have an important role leading to some of the best constraints currently available. In particular, linear drifts in the evolution of the fine-structure constant α, in the ratio μ between the mass of the electron and the mass of the proton, and in the ratio between the mass of the light quarks (up and down) and the quantum chromodynamics (QCD) energy scale $\Lambda_{\rm QCD}$ have been considered. Several groups in the world have pursued effort to constrain such hypothetical linear drifts: at SYRTE [8], NIST [9], Berkeley [10], NPL [11], PTB [12]… The current constraints on the variation of the three constants are at the level of 10^{-16} per year. More recently, searches for a harmonic temporal variation of the constants of Nature using atomic clocks have been performed in Berkeley [13] and SYRTE [14].

Moreover, several astrophysical observations have also been used to search for a temporal evolution of the constants of Nature: observations of quasar absorption lines [15–17], observations of the Cosmic Microwave Background [18], and analysis of the big bang nucleosynthesis [19]. Using a linear interpolation at low redshift, we can compare the order of magnitude of constraints obtained with atomic clocks and using quasar observations. The atomic clock estimations are roughly one order of magnitude more accurate than quasar observations. This comparison implies a linear approximation of the cosmological evolution and implies that no screening mechanism is playing a role around the Earth: a screening

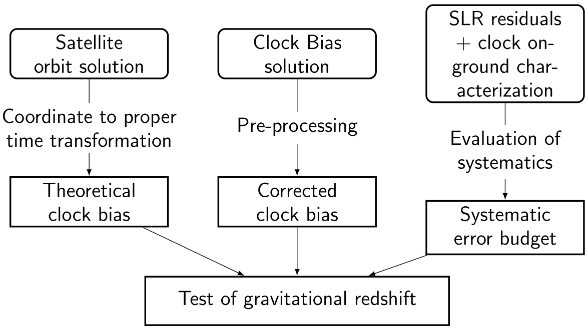

Fig. 1. Data analysis flowchart: as input we use ESOC orbit and clock solution files, SLR residuals as well as clock on-ground characterization. The evaluation of systematics is completely independent of the clock measurements.

mechanism can lead to a situation where deviations from GR at cosmological scales are hidden or strongly reduced on local scales (see, e.g., [20,21]).

In addition to temporal variations of the constants of Nature, one can search for spatial variations. Regarding this, atomic clocks have also been widely used to search for a variation of the constants of Nature with respect to the gravitational potential of the Sun. The idea is to compare two clocks working on different atomic transitions (and therefore differently sensitive to the various constants of physics) located at the same place, and search for periodic variations in their frequency comparison. This kind of tests are also known as null redshift experiments [3]. Several groups in the world have been measuring this effect, which is now constrained at the level of 10^{-6}: SYRTE [8], USNO [22], Berkeley [10], NIST [23]…

The second way to test LPI is to measure the gravitational redshift, which is a direct consequence of the EEP. It was observed for the first time in the Pound–Rebka–Snider experiment [24–27]. In a clock redshift experiment, the fractional frequency difference $z = \Delta\nu/\nu$ between two identical clocks placed at different places in a static gravitational field is measured. The EEP predicts $z = \Delta U/c^2$ for stationary clocks, where ΔU is the gravitational potential difference between the locations of the receiver and the emitter, and c is the velocity of light in vacuum. A simple and convenient formalism to test the gravitational redshift is to introduce a new parameter α defined through [3]:

$$z = \frac{\Delta\nu}{\nu} = (1+\alpha)\frac{\Delta U}{c^2} \tag{1}$$

with $\alpha = 0$ when the EEP is valid. The most precise test of the gravitational redshift until recently had been realized with the Vessot–Levine rocket experiment in 1976, also named the Gravity Probe A (GP-A) experiment [28–30]. The frequency differences between a space-borne hydrogen maser clock and ground hydrogen masers were measured thanks to a continuous two-way microwave link. The gravitational redshift prediction was verified with 1.4×10^{-4} uncertainty, limited by the short duration of the parabolic rocket flight (~ 2 h).

In the next section, we report on the recent test with the clocks of GSAT0201 and GSAT0202 satellites, which improved this limit to 2.5×10^{-5} uncertainty [31]. The future Atomic Clock Ensemble in Space (ACES) experiment [32,33], an ESA/CNES mission, planned to fly on the ISS in 2020, will test the gravitational redshift to around $|\alpha| \leq 3 \times 10^{-6}$. Furthermore, other projects like STE-QUEST propose to test the gravitational redshift at the level of 10^{-7} [34]. Finally, observations with the RadioAstron telescope are expected to reach an uncertainty of the order of 10^{-5} [35].

3. The GREAT experiment

It was proposed in 2015 [5] to use the onboard atomic clocks of the Galileo satellites 5 and 6 (named Doresa and Milena, or GSAT0201 and GSAT0202) to search for violations of the EEP/LPI. These two satellites were launched together on a Soyuz Rocket on 22 August 2014 and because of a technical problem on the launcher's upper stage, they were placed in a non-nominal elliptic orbit. Although the satellites' orbits were adjusted after the launch, they remain elliptical, with each satellite climbing and falling some 8500 km twice per day. The elliptic orbit induces a periodic modulation of the gravitational redshift at orbital period (around 13 h, see Fig. 5), while the good stability of recent GNSS clocks allows us to measure this periodic modulation to a new level of uncertainty. The Galileo 5 and 6 satellites, with their large eccentricity ($e = 0.162$) and onboard passive hydrogen-maser (PHM) clocks, are hence perfect candidates to perform this test. Contrary to the GP-A experiment, it is possible to integrate the signal over a long duration, therefore improving the statistics. Moreover, a specific ILRS (International Laser Ranging Service) campaign took place during the years 2016–2017 [36]. Satellite Laser Ranging (SLR) data are used for a characterization of systematic effects.

The analysis covers three years of data and is reported in [31] (see Fig. 1 for a summary of the data analysis). The satellite orbits and clock bias are computed by the ESA/ESOC centre, using the latest models for clocks and satellite dynamics. Satellite orbits and time epochs are calculated in the Geocentric Celestial Reference System (GCRS) thanks to the Standards

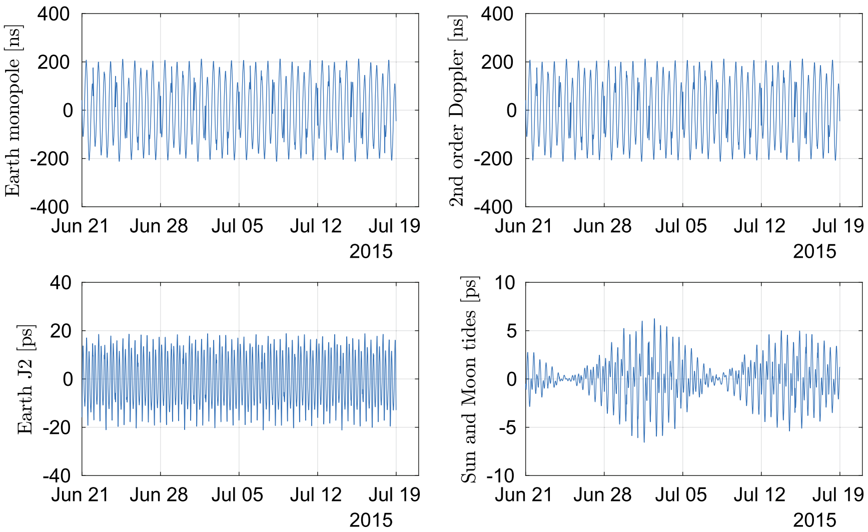

Fig. 2. GR prediction of the proper time of the onboard clock showing only the periodic term, which can be split into two contributions: gravitational redshift due to the Earth's potential and other bodies, and second-order Doppler effect. The Earth monopole contribution and second-order Doppler effect lead to a similar periodic effect at the orbital period, with peak-to-peak variation of 400 ns. The Earth flatness leads to a 40-ps peak-to-peak periodic effect at twice the orbital frequency. Tidal effects from the Moon and the Sun lead to a periodic signal of around 12 ps peak to peak. A daily linear fit is removed from the model just for visualization.

of Fundamental Astronomy (SOFA) routines [37]. Then, we calculate the theoretical proper time of the onboard clock τ_{GR} – predicted by GR – by integrating the coordinate time to proper time transformation:

$$\tau_{\mathrm{GR}} = \int \frac{\mathrm{d}\tau}{\mathrm{d}t}\mathrm{d}t = \int \left[1 - \frac{v^2}{2c^2} - \frac{U_{\mathrm{E}} + U_{\mathrm{T}}}{c^2}\right]\mathrm{d}t \tag{2}$$

where τ and t are the proper time and the coordinate time (geocentric coordinate time TCG) of the clock, respectively, c is the velocity of light in a vacuum, v is the velocity of the clock in the GCRS. Also, U_{E} is the Newtonian gravitational potential of the Earth at the location of the satellite given by

$$U_{\mathrm{E}} = \frac{GM}{r} + \frac{GMR_0^2 J_2}{2r^3}\left(1 - 3\cos^2\theta\right) \tag{3}$$

where G is the gravitational constant, M, R_0, and J_2 are the mass, the equatorial radius and the zonal coefficient of order 2 of the Earth, respectively, and r and θ are the distance from the center of the Earth and the co-latitude of the satellite, respectively. U_{T} is the tidal potential due to external bodies [38]

$$U_{\mathrm{T}} = \sum_A GM_A\left[\frac{1}{|\boldsymbol{r} - \boldsymbol{r}_A|} - \frac{1}{|\boldsymbol{r}_A|} - \frac{\boldsymbol{r}\cdot\boldsymbol{r}_A}{|\boldsymbol{r}_A|^3}\right] \tag{4}$$

where M_A is the mass of external body A, and $\boldsymbol{r}$ and $\boldsymbol{r}_A$ are respectively the position vectors of the satellite and external body A in the geocentric frame. We take into account the Moon and the Sun, while other bodies can be neglected.

The main gravitational effect is the sum of a linear and a periodic term, which amounts to 400 ns peak to peak (see Fig. 5). Contributions of the periodic terms are given in Fig. 2 for a subsample of data.

The deviation of the proper time from the GR prediction, τ_{LPI}, is quantified by the LPI violation parameter α as given in (1) and proportional to the gravitational part of the coordinate to proper time transformation:

$$\tau_{\mathrm{LPI}} = -\alpha\int\frac{U_{\mathrm{E}} + U_{\mathrm{T}}}{c^2}\mathrm{d}t \tag{5}$$

The raw clock bias τ_{ESOC} from the ESOC clock solution contains a large drift of the order of 34 µs d^{-1}, which is present most of the time (see Fig. 3). The linear part of the relativistic redshift between the Galileo clocks and a ground clock is ≈ 40 µs d^{-1} assuming a nominal 10.23 MHz frequency. However, each PHM clock is also affected by an intentional frequency offset (≈ -6 µs d^{-1}) to this nominal frequency, which explains the observed drift. Additionally, after each activation, the clock retraces to the nominal frequency with an accuracy not better than ± 0.18 µs d^{-1}. We account for this unknown frequency offset (together with the known ≈ 34 µs d^{-1}) by removing from the clock bias a daily linear fit (DLF), which can be written in the form

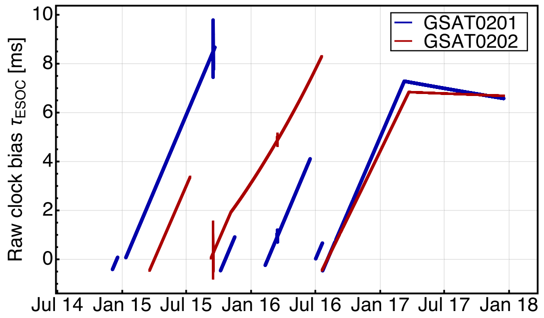

Fig. 3. Raw clock bias τ_{ESOC}, as read in the ESOC clock solution file.

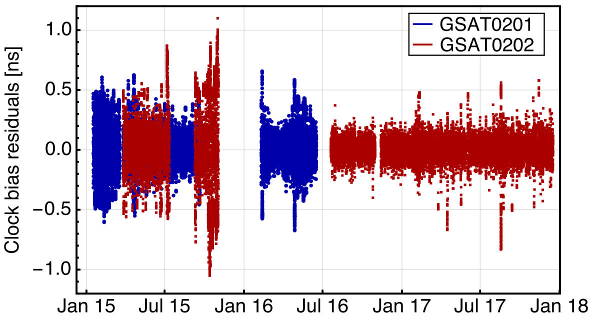

Fig. 4. Clock bias pre-fit residuals are obtained by removing from the corrected clock bias τ_{corr} a daily linear fit.

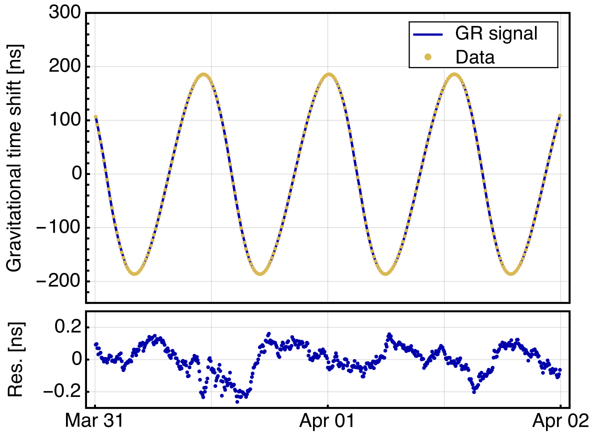

Fig. 5. GR prediction, clock data (after removal of a daily linear fit) and residuals are shown for 2 days from 31 March 2016. The peak to peak effect is around 400 ns; therefore, the model and systematic effects at orbital period should be controlled down to 4 ps in order to have a 1×10^{-5} uncertainty on the LPI violation parameter α.

$$\tau_{\mathrm{DLF}} = \sum_{i=1}^{N} f_i(t)(a_i + b_i t) \tag{6}$$

where N is the number of days in the data, a_i and b_i are the clock offset and linear drift for day i, respectively, and $f_i(t)$ is equal to 1 for day i, and 0 otherwise. The obtained clock bias pre-fit residuals are shown on Fig. 4.

The data analysis contains 359 days of data from GSAT0201 and 649 days of data from GSAT0202, spanning from January 2015 to December 2017. The raw clock bias τ_{ESOC} is corrected to account for the full GR prediction given in Eq. (2), providing the corrected clock bias τ_{corr}. The data analysis is performed in three steps. First, we fit a model for the stochastic noise to the corrected clock bias residuals. In a second step, we fit the model defined from equations (5) and (6) to the corrected clock bias by using a Monte Carlo approach, using the stochastic noise model estimated in the first step. This gives us the fitted value for α as well as an estimation of its statistical uncertainty. In a third step, we estimate the systematic uncertainty by considering the main sources of systematic uncertainties: effects of magnetic field, of temperature and mismodelling of the orbital motion of the satellites. A detailed description of these procedures is given in [31].

Finally, by analysing 1008 days of data from the two eccentric Galileo satellites, GSAT0201 and GSAT0202, and through a careful analysis of systematic effects, we were able to improve the gravitational redshift test done by GP-A in 1976 by a factor 5.6, down to:

$$\alpha = 0.19 \pm 2.48 \times 10^{-5}$$

Our result is at the lower edge of the predicted sensitivity in [5]. Moreover, this result has been confirmed by an independent analysis in [39], with a slightly lower accuracy.

At this point, the main residual limiting factor is the uncertainty due to the magnetic field variations, which cannot be overcome without more information about the clock sensitivity (e.g., directional dependence) and the actual local magnetic field after, e.g., shielding from the satellite itself. The three main uncertainties, i.e. statistical, orbit and magnetic field, are of the same order. Therefore, envisaging a potential future mission of the same type, it would be of interest to improve these three aspects of the experiment: a more stable clock to have better statistics, a careful shielding, modelling or measurement of the magnetic field, and a careful modelling or measurement of non gravitational accelerations. Also, increasing the signal (higher ellipticity, lower perigee) would improve the test significantly (see, e.g., the STE-QUEST proposal [34]). Finally, a two-way link would strongly reduce the effect of orbit determination uncertainties (see, e.g., the ACES proposal [32,33]).

Acknowledgements

We acknowledge financial support from the European Space Agency (ESA) within the GREAT (Galileo gravitational Redshift Experiment with eccentric sATellites) project, from Paris Observatory/GPhys specific action and from Generalitat Valenciana APOSTD2017.

References

[1] A. Einstein, Über das Relativitäts Prinzip und die aus denselben gezogenen Folgerungen, Jahrb. d. Rad. u. El. 4 (1907) 411–462.

[2] K.S. Thorne, D.L. Lee, A.P. Lightman, Foundations for a theory of gravitation theories, Phys. Rev. D 7 (12) (1973) 3563–3578, https://doi.org/10.1103/PhysRevD.7.3563.

[3] C.M. Will, The confrontation between general relativity and experiment, Living Rev. Relativ. 17 (2014) 4, https://doi.org/10.12942/lrr-2014-4.

[4] C.M. Will, Theory and Experiment in Gravitational Physics, Cambridge University Press, 1993.

[5] P. Delva, A. Hees, S. Bertone, E. Richard, P. Wolf, Test of the gravitational redshift with stable clocks in eccentric orbits: application to Galileo satellites 5 and 6, Class. Quantum Gravity 32 (23) (2015) 232003, https://doi.org/10.1088/0264-9381/32/23/232003.

[6] T. Damour, Theoretical aspects of the equivalence principle, Class. Quantum Gravity 29 (18) (2012) 184001, https://doi.org/10.1088/0264-9381/29/18/184001.

[7] J.-P. Uzan, Varying constants, gravitation and cosmology, Living Rev. Relativ. 14 (2) (2011), https://doi.org/10.12942/lrr-2011-2.

[8] J. Guéna, M. Abgrall, D. Rovera, P. Rosenbusch, M.E. Tobar, P. Laurent, A. Clairon, S. Bize, Improved tests of local position invariance using ^{87}Rb and ^{133}Cs fountains, Phys. Rev. Lett. 109 (8) (2012) 080801, https://doi.org/10.1103/PhysRevLett.109.080801.

[9] T. Rosenband, D.B. Hume, P.O. Schmidt, C.W. Chou, A. Brusch, L. Lorini, W.H. Oskay, R.E. Drullinger, T.M. Fortier, J.E. Stalnaker, S.A. Diddams, W.C. Swann, N.R. Newbury, W.M. Itano, D.J. Wineland, J.C. Bergquist, Frequency ratio of Al^+ and Hg^+ single-ion optical clocks; metrology at the 17th decimal place, Science 319 (5871) (2008) 1808–1812, https://doi.org/10.1126/science.1154622.

[10] N. Leefer, C.T.M. Weber, A. Cingöz, J.R. Torgerson, D. Budker, New limits on variation of the fine-structure constant using atomic dysprosium, Phys. Rev. Lett. 111 (6) (2013) 060801, https://doi.org/10.1103/PhysRevLett.111.060801.

[11] R.M. Godun, P.B.R. Nisbet-Jones, J.M. Jones, S.A. King, L.A.M. Johnson, H.S. Margolis, K. Szymaniec, S.N. Lea, K. Bongs, P. Gill, Frequency ratio of two optical clock transitions in $^{171}Yb^+$ and constraints on the time variation of fundamental constants, Phys. Rev. Lett. 113 (21) (2014) 210801, https://doi.org/10.1103/PhysRevLett.113.210801.

[12] N. Huntemann, B. Lipphardt, C. Tamm, V. Gerginov, S. Weyers, E. Peik, Improved limit on a temporal variation of m_p/m_e from comparisons of Yb^+ and Cs atomic clocks, Phys. Rev. Lett. 113 (21) (2014) 210802, https://doi.org/10.1103/PhysRevLett.113.210802.

[13] K. Van Tilburg, N. Leefer, L. Bougas, D. Budker, Search for ultralight scalar dark matter with atomic spectroscopy, Phys. Rev. Lett. 115 (1) (2015) 011802, https://doi.org/10.1103/PhysRevLett.115.011802.

[14] A. Hees, J. Guéna, M. Abgrall, S. Bize, P. Wolf, Searching for an oscillating massive scalar field as a dark matter candidate using atomic hyperfine frequency comparisons, Phys. Rev. Lett. 117 (6) (2016) 061301, https://doi.org/10.1103/PhysRevLett.117.061301.

[15] J.K. Webb, M.T. Murphy, V.V. Flambaum, V.A. Dzuba, J.D. Barrow, C.W. Churchill, J.X. Prochaska, A.M. Wolfe, Further evidence for cosmological evolution of the fine structure constant, Phys. Rev. Lett. 87 (9) (2001) 091301, https://doi.org/10.1103/PhysRevLett.87.091301.

[16] J.K. Webb, J.A. King, M.T. Murphy, V.V. Flambaum, R.F. Carswell, M.B. Bainbridge, Indications of a spatial variation of the fine structure constant, Phys. Rev. Lett. 107 (19) (2011) 191101, https://doi.org/10.1103/PhysRevLett.107.191101.

[17] R. Srianand, H. Chand, P. Petitjean, B. Aracil, Limits on the time variation of the electromagnetic fine-structure constant in the low energy limit from absorption lines in the spectra of distant quasars, Phys. Rev. Lett. 92 (12) (2004) 121302, https://doi.org/10.1103/PhysRevLett.92.121302.

[18] P. a, R. Ade, N. Aghanim, C. Armitage-Caplan, M. Arnaud, M. Ashdown, F. Atrio-Barandela, J. Aumont, C. Baccigalupi, A.J. Banday, R.B. Barreiro, J.G. Bartlett, E. Battaner, K. Benabed, A. Benoît, A. Benoit-Lévy, J.-P. Bernard, M. Bersanelli, P. Bielewicz, J. Bobin, J.J. Bock, A. Bonaldi, J.R. Bond, J. Borrill, F.R. Bouchet, M. Bridges, M. Bucher, C. Burigana, R.C. Butler, E. Calabrese, B. Cappellini, J.-F. Cardoso, A. Catalano, A. Challinor, A. Chamballu, R.-R. Chary, X. Chen, H.C. Chiang, L.-Y. Chiang, P.R. Christensen, S. Church, D.L. Clements, S. Colombi, L.P.L. Colombo, F. Couchot, A. Coulais, B.P. Crill, A. Curto, F. Cuttaia, L. Danese, R.D. Davies, R.J. Davis, P. de Bernardis, A. de Rosa, G. de Zotti, J. Delabrouille, J.-M. Delouis, F.-X. Désert, C. Dickinson, J.M. Diego, K. Dolag, H. Dole, S. Donzelli, O. Doré, M. Douspis, J. Dunkley, X. Dupac, G. Efstathiou, F. Elsner, T.A. Enßlin, H.K. Eriksen, F. Finelli, O. Forni, M. Frailis, A.A. Fraisse, E. Franceschi, T.C. Gaier, S. Galeotta, S. Galli, K. Ganga, M. Giard, G. Giardino, Y. Giraud-Héraud, E. Gjerløw, J. González-Nuevo, K.M. Górski, S. Gratton, A. Gregorio, A. Gruppuso, J.E. Gudmundsson, J. Haissinski, J. Hamann, F.K. Hansen, D. Hanson, D. Harrison, S. Henrot-Versillé, C. Hernández-Monteagudo, D. Herranz, S.R. Hildebrandt, E. Hivon, M. Hobson, W.A. Holmes, A. Hornstrup, Z. Hou, W. Hovest, K.M. Huffenberger, A.H. Jaffe, T.R. Jaffe, J. Jewell, W.C. Jones, M. Juvela, E. Keihänen, R. Keskitalo, T.S. Kisner, R. Kneissl, J. Knoche, L. Knox, M. Kunz, H. Kurki-Suonio, G. Lagache, A. Lähteenmäki, J.-M. Lamarre, A. Lasenby, M. Lattanzi, R.J. Laureijs, C.R. Lawrence, S. Leach, J.P. Leahy, R. Leonardi, J. León-Tavares, J. Lesgourgues, A. Lewis, M. Liguori, P.B. Lilje, M. Linden-Vørnle, M. López-Caniego, P.M. Lubin, J.F. Macías-Pérez, B. Maffei, D. Maino, N. Mandolesi, M. Maris, D.J. Marshall, P.G. Martin,

E. Martínez-González, S. Masi, M. Massardi, S. Matarrese, F. Matthai, P. Mazzotta, P.R. Meinhold, A. Melchiorri, J.-B. Melin, L. Mendes, E. Menegoni, A. Mennella, M. Migliaccio, M. Millea, S. Mitra, M.-A. Miville-Deschênes, A. Moneti, L. Montier, G. Morgante, D. Mortlock, A. Moss, D. Munshi, J.A. Murphy, P. Naselsky, F. Nati, P. Natoli, C.B. Netterfield, H.U. Nørgaard-Nielsen, F. Noviello, D. Novikov, I. Novikov, I.J. O'Dwyer, S. Osborne, C.A. Oxborrow, F. Paci, L. Pagano, F. Pajot, R. Paladini, D. Paoletti, B. Partridge, F. Pasian, G. Patanchon, D. Pearson, T.J. Pearson, H.V. Peiris, O. Perdereau, L. Perotto, F. Perrotta, V. Pettorino, F. Piacentini, M. Piat, E. Pierpaoli, D. Pietrobon, S. Plaszczynski, P. Platania, E. Pointecouteau, G. Polenta, N. Ponthieu, L. Popa, T. Poutanen, G.W. Pratt, G. Prézeau, S. Prunet, J.-L. Puget, J.P. Rachen, W.T. Reach, R. Rebolo, M. Reinecke, M. Remazeilles, C. Renault, S. Ricciardi, T. Riller, I. Ristorcelli, G. Rocha, C. Rosset, G. Roudier, M. Rowan-Robinson, J.A. Rubiño-Martín, B. Rusholme, M. Sandri, D. Santos, M. Savelainen, G. Savini, D. Scott, M.D. Seiffert, E.P.S. Shellard, L.D. Spencer, J.-L. Starck, V. Stolyarov, R. Stompor, R. Sudiwala, R. Sunyaev, F. Sureau, D. Sutton, A.-S. Suur-Uski, J.-F. Sygnet, J.A. Tauber, D. Tavagnacco, L. Terenzi, L. Toffolatti, M. Tomasi, M. Tristram, M. Tucci, J. Tuovinen, M. Türler, G. Umana, L. Valenziano, J. Valiviita, B.V. Tent, P. Vielva, F. Villa, N. Vittorio, L.A. Wade, B.D. Wandelt, I.K. Wehus, M. White, S.D.M. White, A. Wilkinson, D. Yvon, A. Zacchei, A. Zonca, Planck 2013 results. XVI. Cosmological parameters, Astron. Astrophys. 571 (2014) A16, https://doi.org/10.1051/0004-6361/201321591.

[19] P.P. Avelino, S. Esposito, G. Mangano, C.J.A.P. Martins, A. Melchiorri, G. Miele, O. Pisanti, G. Rocha, P.T.P. Viana, Early-universe constraints on a time-varying fine structure constant, Phys. Rev. D 64 (10) (2001) 103505, https://doi.org/10.1103/PhysRevD.64.103505.

[20] J. Khoury, A. Weltman, Chameleon fields: awaiting surprises for tests of gravity in space, Phys. Rev. Lett. 93 (17) (2004) 171104, https://doi.org/10.1103/PhysRevLett.93.171104.

[21] J. Khoury, A. Weltman, Chameleon cosmology, Phys. Rev. D 69 (4) (2004) 044026, https://doi.org/10.1103/PhysRevD.69.044026.

[22] S. Peil, S. Crane, J.L. Hanssen, T.B. Swanson, C.R. Ekstrom, Tests of local position invariance using continuously running atomic clocks, Phys. Rev. A 87 (1) (2013) 010102, https://doi.org/10.1103/PhysRevA.87.010102.

[23] N. Ashby, T.P. Heavner, S.R. Jefferts, T.E. Parker, A.G. Radnaev, Y.O. Dudin, Testing local position invariance with four cesium-fountain primary frequency standards and four NIST hydrogen masers, Phys. Rev. Lett. 98 (7) (2007) 070802, https://doi.org/10.1103/PhysRevLett.98.070802.

[24] R.V. Pound, G.A. Rebka, Apparent weight of photons, Phys. Rev. Lett. 4 (7) (1960) 337–341, https://doi.org/10.1103/PhysRevLett.4.337.

[25] R.V. Pound, G.A. Rebka, Gravitational red-shift in nuclear resonance, Phys. Rev. Lett. 3 (9) (1959) 439–441, https://doi.org/10.1103/PhysRevLett.3.439.

[26] R.V. Pound, G.A. Rebka, Resonant absorption of the 14.4-keV γ ray from 0.10-μsec Fe^{57}, Phys. Rev. Lett. 3 (12) (1959) 554–556, https://doi.org/10.1103/PhysRevLett.3.554.

[27] R.V. Pound, J.L. Snider, Effect of gravity on gamma radiation, Phys. Rev. 140 (3B) (1965) B788–B803, https://doi.org/10.1103/PhysRev.140.B788.

[28] R.F.C. Vessot, M.W. Levine, E.M. Mattison, E.L. Blomberg, T.E. Hoffman, G.U. Nystrom, B.F. Farrel, R. Decher, P.B. Eby, C.R. Baugher, J.W. Watts, D.L. Teuber, F.D. Wills, Test of relativistic gravitation with a space-borne hydrogen maser, Phys. Rev. Lett. 45 (26) (1980) 2081–2084, https://doi.org/10.1103/PhysRevLett.45.2081.

[29] R.F.C. Vessot, M.W. Levine, A test of the equivalence principle using a space-borne clock, Gen. Relativ. Gravit. 10 (3) (1979) 181–204, https://doi.org/10.1007/BF00759854.

[30] R.F.C. Vessot, Clocks and spaceborne tests of relativistic gravitation, Adv. Space Res. 9 (9) (1989) 21–28, https://doi.org/10.1016/0273-1177(89)90004-5.

[31] P. Delva, N. Puchades, E. Schönemann, F. Dilssner, C. Courde, S. Bertone, F. Gonzalez, A. Hees, C. Le Poncin-Lafitte, F. Meynadier, R. Prieto-Cerdeira, B. Sohet, J. Ventura-Traveset, P. Wolf, Gravitational redshift test using eccentric Galileo satellites, Phys. Rev. Lett. 121 (2018) 231101, https://doi.org/10.1103/PhysRevLett.121.231101, https://link.aps.org/doi/10.1103/PhysRevLett.121.231101.

[32] L. Cacciapuoti, C. Salomon, Space clocks and fundamental tests: the ACES experiment, Eur. Phys. J. Spec. Top. 172 (1) (2009) 57–68, https://doi.org/10.1140/epjst/e2009-01041-7.

[33] F. Meynadier, P. Delva, C. le Poncin-Lafitte, C. Guerlin, P. Wolf, Atomic clock ensemble in space (ACES) data analysis, Class. Quantum Gravity 35 (3) (2018) 035018, https://doi.org/10.1088/1361-6382/aaa279.

[34] B. Altschul, Q.G. Bailey, L. Blanchet, K. Bongs, P. Bouyer, L. Cacciapuoti, S. Capozziello, N. Gaaloul, D. Giulini, J. Hartwig, others, quantum tests of the Einstein equivalence principle with the STE–QUEST space mission, Adv. Space Res. 55 (1) (2015) 501–524, https://doi.org/10.1016/j.asr.2014.07.014.

[35] D.A. Litvinov, V.N. Rudenko, A.V. Alakoz, U. Bach, N. Bartel, A.V. Belonenko, K.G. Belousov, M. Bietenholz, A.V. Biriukov, R. Carman, et al., Probing the gravitational redshift with an Earth-orbiting satellite, Phys. Lett. A (2018), https://doi.org/10.1016/j.physleta.2017.09.014.

[36] P. Delva, M. Aimar, D. Albanese, S. Bertone, C. Courde, F. Deleflie, P. Exertier, D. Feraudy, A. Hees, S. Herrmann, et al., An SLR campaign on Galileo satellites 5 and 6 for a test of the gravitational redshift – the GREAT experiment, in: Proceedings of the ILRS Technical Workshop, Matera, Italy, October, 2015, 2016, pp. 26–30.

[37] IAU SOFA Board, IAU SOFA Software Collection, issue 2016-05-03, http://www.iausofa.org.

[38] P. Wolf, G. Petit, Relativistic theory for clock syntonization and the realization of geocentric coordinate times, Astron. Astrophys. 304 (1995) 653.

[39] S. Herrmann, F. Finke, M. Lülf, O. Kichakova, D. Puetzfeld, D. Knickmann, M. List, B. Rievers, G. Giorgi, C. Günther, H. Dittus, R. Prieto-Cerdeira, F. Dilssner, F. Gonzalez, E. Schönemann, J. Ventura-Traveset, C. Lämmerzahl, Test of the gravitational redshift with Galileo satellites in an eccentric orbit, Phys. Rev. Lett. 121 (2018) 231102, https://doi.org/10.1103/PhysRevLett.121.231102.